Examination of targeted, activity-dependent spinal stimulation in a rat model of spinal cord injury

Kristen Drummey

A thesis
submitted in partial fulfillment of the
requirements for the degree of

Master of Science

University of Washington
2023

Committee:
Steve Perlmutter
Jane Sullivan
John Tuthill

Program Authorized to Offer Degree:
Neuroscience

University of Washington

Abstract

Examination of targeted, activity-dependent spinal stimulation in a rat model of spinal cord injury

Kristen Drummey

Chair of the Supervisory Committee:
Steve Perlmutter
Department of Physiology and Biophysics

Spinal cord injuries (SCIs) cause debilitating motor and sensory impairments that can significantly impact patients' quality of life. Although an estimated 300,000 people in the United States are living with a spinal cord injury, there are few available treatments for chronic injuries beyond physical and occupational therapy. Even after injury, the spinal cord has an innate ability for plasticity that can promote spontaneous recovery and be harnessed with therapeutic interventions to improve functional outcomes for patients. Previous work has shown that targeted, activity-dependent electrical stimulation of the spine in an animal model improves functional outcomes greater than open-loop electrical stimulation or physical retraining alone. However, the mechanism by which this targeted stimulation works and whether it is promoting plasticity in particular descending pathways remains unclear. We hypothesized that this therapy paradigm targets descending cortical projections to the spinal cord and that electrophysiological recordings of the motor cortex and anatomical tracing of this corticospinal tract would reveal changes after injury and with therapy. Unfortunately, we were unable to answer these questions, but new knowledge of technical limitations will hopefully provide a baseline for future pursuance of this research.

Table of Contents

Chapter 1

Background

1.1 Introduction

Spinal cord injury (SCI) occurs when the nervous tissue of the spinal cord is damaged or destroyed, altering the transmission potential and efficiency of descending motor pathways from the brain and ascending sensory pathways from the limbs (Ahuja et. al., 2017). SCIs are incredibly variable, with level of injury, injury cause, and injury type causing a wide range of primary sensory and motor impairments and additional secondary effects that can severely impact patients' quality of life (Barbiellini et. al., 2022; Noreau et. al., 2014). Although there are numerous novel therapy types under investigation (Hu et. al., 2023), currently available treatment options are often invasive and may provide limited benefits depending on injury level and severity (Marquez-Chin & Popovic, 2020).

Although ascending and descending spinal pathways can be severely damaged after SCI, these pathways and their connections in the cord maintain the capacity for plasticity after injury (Anderson et. al., 2022; Raineteau & Schwab, 2001). Animal models with partial or full transection injuries, in which spinal pathways are partially or completely severed, show some capacity for spontaneous recovery and recovered movement (Vipin et. al., 2016). Patients with functionally complete SCIs also show some level of spontaneous recovery, suggesting that innate plasticity in preserved neuronal connections can be leveraged to promote more complete recovery after injury (Steeves et. al., 2011).

Targeted, activity-dependent spinal stimulation (TADSS), in combination with physical retraining, was developed in order to take advantage of this innate plasticity. TADSS uses an activity signal from the injured forelimb to deliver electrical stimulation to the spinal cord within the timescale necessary for induction of spike timing-dependent plasticity (McPherson, et. al., 2015, Bi & Poo, 1998). TADSS is more effective at promoting behavioral recovery in injured animals than stimulation delivered without an activity trigger or physical rehabilitation alone (McPherson et. al., 2015). The

effectiveness of TADSS suggests that SCI therapies based on neuronal plasticity paradigms are a promising path toward improved therapies in human patients.

1.2 SCI pathophysiology and epidemiology

Traumatic SCIs cause a chain reaction of acute, subacute, and chronic changes in the spinal cord. During and immediately after injury, mechanical disruption at the site of injury can cause immediate cell damage and death, and hemorrhaging due to disrupted blood vessels can both increase mechanical displacement of the cord and deprive spared tissue of necessary oxygen. In the acute stages following injury, inflammation increases in the cord as immune cells invade the area. The release of inflammatory cytokines and apoptotic signals from dying cells can damage cells that were spared by the injury itself. Eventually, as the injured cord moves into a more chronic state, a glial scar may form around the site of injury. The scar typically contains inhibitory signals that prevent processes from branching through the scar, limiting the potential connectivity of the spinal cord above and below the injury site (Ahuja et. al., 2017).

Despite sometimes extensive cell death and the presence of inhibitory scarring, the injured cord retains some capacity for plasticity. Numerous studies have shown that the injured cord in animal subjects and human patients is capable of producing some spontaneous recovery in the absence of interventions such as physical therapy (Raineteau & Schwab, 2001; Vipin et. al., 2016). Additionally, several studies have shown that application of interventions such as electrical stimulation, chemical modulation with neurotransmitters or neurotrophic factors, or weight-assisted physical retraining can promote significant functional recovery in subjects with SCIs (Asboth et. al., 2018; Samejima et. al. 2022; Yang et. al., 2022).

Although there are a wide variety of promising therapeutic approaches for chronic SCI currently under investigation, very few are approved for clinical use or widely available to the many patients with a SCI. In the United States alone, nearly 18,000 people experience a new SCI each year and over 300,000 people are currently living with an SCI. The lifetime costs for individuals with a SCI vary depending on age at injury and injury severity, but in all cases run well into the millions of

dollars (National Spinal Cord Injury Statistical Center, 2023). Individuals with SCIs have a significantly reduced lifespan compared to individuals without SCI, and individuals living with these injuries may face significant challenges in their daily life. Mobility impairment is often the most cited impact, but additional difficulties with neuropathic pain, sexual dysfunction, incontinence, muscle spasticity, and repetitive infections can also severely undermine patients' quality of life (Noreau et. al., 2014).

1.3 Current treatments for SCI

Currently available treatments for individuals with chronic SCI are relatively limited. The primary and most accessible treatment is physical retraining, which often employs a combination of physical and occupational therapies. These therapies are a critical intervention for preventing or mitigating secondary complications from SCI, such as muscle atrophy in or pressures sores on mobility-impaired limbs, and has an added benefit of improving patients' cardiovascular health, but have limited impact on overall functional recovery (Gómara-Toldrà, et. al., 2014).

Functional electrical stimulation (FES) is a less common therapeutic that uses electrical pulses, typically delivered via electrodes implanted in the muscles. FES is effective at improving behavioral function but is limited in its use; since it is essentially bypassing the spine and directly activating the muscles necessary for a particular action, it typically is only effective when turned on, and mobility improvements cease when the stimulation is turned off. Current iterations of FES also require an invasive implantation procedure, and the technical requirements for mediating stimulation amplitude and timing can cause undue burden on patients and caregivers (Marquez-Chin & Popovic, 2020).

Numerous novel therapeutics are currently under investigation, with research typically falling into one of two categories: increasing plasticity of preserved circuitry following injury, and regenerating or replacing damaged spinal pathways. One kind of novel therapeutic involves delivering electrical stimulation directly to the spine in an attempt to return some of the excitability lost after injury and promote plasticity at spared spinal circuits. Two such therapeutics, epidural

electrical stimulation (EES), which delivers stimulation through epidural arrays implanted in the spinal cord, and transcutaneous spinal stimulation, which delivers stimulation through a non-invasive contact on the skin, hold promise as advanced methods of increasing excitability in the injured spinal cord (Anderson et. al., 2022; Samejima et. al., 2022).

Stem cell grafts and delivery of transcription factors via methods such as viral injection are also being investigated as methods for generating new axonal growth and rebuilding pathways that were destroyed by the injury. Although all of these treatment avenues hold promise, none are currently approved for use in humans and few examine the effects of multiple interventions delivered simultaneously (Hachem et. al., 2017).

1.4 Targeted, activity-dependent spinal stimulation (TADSS)

Targeted, activity-dependent spinal stimulation (TADSS), previously developed in the lab, is a novel therapy paradigm designed to take advantage of innate plasticity in the injured spine. Unlike typical implementations of FES, TADSS uses a closed-loop system to deliver electrical stimulation directly into the spinal cord while animals are performing a motor task. TADSS uses electromyography (EMG) signals from muscles in the injured forelimb to trigger stimulation in the spine in an effort to direct plasticity during functionally relevant movement. Indeed, previous work in the lab showed that TADSS improves behavioral outcomes in injured rats greater than open-loop stimulation combined with physical retraining or physical retraining alone (McPherson et. al., 2015).

Although TADSS holds promise as a refined approach to stimulation therapy after SCI, it is currently limited in several ways. Primarily among those is that, as it is currently designed, TADSS requires EMG input in order to trigger stimulation. It is an effective therapy in moderately injured rats who have retained some volitional forelimb movement and function, but has little use in rats with severe injuries who have little to no movement in their injured forelimb.

Additionally, although we know that TADSS is more effective at improving behavioral outcomes than open-loop stimulation or retraining alone, the mechanism by which TADSS affects behavioral recovery is not entirely clear. We hypothesize that TADSS is enhancing plasticity at

preserved corticospinal tract (CST) connections in a spike-timing dependent manner. In our hands, the delay between EMG activity and spinal stimulation is 10ms, well within the spike timing-dependent plasticity (STDP) window of 20-25ms (Bi & Poo, 1998; McPherson et. al., 2015). Additionally, improvement in tasks that require fine motor control of the forelimb suggest that TADSS is strengthening connections of preserved CST fibers, known to be important for mediating dextrous movement in the digits and forelimb (Lemon, 2008). However, despite reasonable hypotheses as to how TADSS is mediating functional recovery, the true underlying mechanism remains unknown.

1.5 Questions and hypotheses

We attempted to examine whether and how TADSS affects the CST through two techniques: electrophysiological recordings using electrocorticography (ECoG) and tetrode arrays, and anatomical tracing using adeno-associated viruses (AAVs). For electrophysiological recordings, we aimed to determine whether ECoG could detect oscillatory changes around volitional forelimb movement that could be used to trigger TADSS instead of EMG. We also attempted to use tetrodes to record single units in MCtx to determine whether putative projection cells had a different activity pattern before and after injury, and before and after TADSS.

In addition to electrophysiological recordings, we also attempted to use viral tracing to determine the anatomical impacts of TADSS on the CST. The viruses used were designed to carry transcription factors that had been previously shown to improve sprouting in preserved axons following injury (Venkatesh et. al., 2020), but did not induce any improvement in behavioral function (Kramer et. al., 2021). We hypothesized that TADSS combined with administration of these transcription factors would help direct connections of newly sprouted axons and improve behavioral function greater than TADSS alone.

Chapter 2

Assessment of motor cortex activity after spinal cord injury

2.1 Abstract

Targeted, activity-dependent spinal stimulation (TADSS) is an effective therapy model for improving behavioral recovery in rats after spinal cord injury. However, it is unclear whether TADSS is mediating these changes via the corticospinal tract (CST) and whether directly targeting this descending pathway would produce more effective, functionally relevant plasticity at connections in the injured spinal cord. Additionally, TADSS is limited by its use of electromyography (EMG) signals as a trigger for stimulation, a trigger that is not available in severely injured rats with limited forelimb muscle movement. To determine how motor cortex (MCtx) activity changes after spinal cord injury and with TADSS therapy, we created custom electrocorticography (ECoG) and tetrode arrays in order to examine the population level activity of and single unit activity in the MCtx during a skilled reaching task. Unfortunately, technical limitations prevented us from drawing definitive conclusions about the nature of MCtx activity during this task. The utility of ECoG as a trigger for TADSS therapy and the activity of neurons in MCtx after injury and during therapy remain open questions.

2.2 Background

Targeted, activity-dependent spinal stimulation (TADSS) improves functional recovery in an animal model greater than open-loop spinal stimulation or physical retraining alone. We believe that TADSS is mediating this improvement specifically via plasticity at corticospinal tract (CST) axons in the spinal cord. The CST, which originates in layer V of MCtx and sends projections directly to the spinal cord, is important for mediating fine forelimb motor skills in the

rat and in humans (Lemon, 2008). Additionally, TADSS stimulation is delivered at a timescale sufficient to induce spike timing-dependent plasticity at putative CST synapses (Bi & Poo, 1998; McPherson et. al. 2015). However, to date, this hypothesis of the mechanism of TADSS is unconfirmed.

Additionally, although TADSS has proven effective at improving motor recovery in skilled reaching tasks after injury, its use is limited to animals with mild to moderate injury levels. Since TADSS uses closed-loop stimulation triggered off of muscle activity in the injured forelimb, animals with severe, motor-complete injuries are not candidates for TADSS due to their impaired forelimb having little to no volitional muscle contraction.

Changes in motor cortex (MCtx) activity after spinal cord injury are relatively unexplored. Magnetic resonance imaging in non-human primates with SCI has shown that there are bilateral changes in MCtx activity that vary depending on the period of time after injury and with retraining (Nishimura & Isa, 2012). To our knowledge, assessment of MCtx activity changes after SCI have not been categorized in the rat. It is also unclear whether and how a spinal stimulation-based therapy such as TADSS would impact activity in the MCtx.

In order to determine whether TADSS induces plasticity at CST connections and to expand the therapeutic potential of this intervention, we decided to first examine the effects of chronic SCI on MCtx signaling. We attempted to quantify these signals using both electrocorticography (ECoG) and tetrode arrays to examine both large cortical oscillations and more localized single units. Unfortunately, technical issues prevented any clear results, and the role of the CST in TADSS recovery and the impacts of SCI on the rat MCtx remain unresolved.

2.3 Methods

2.3.1 Animals

Female Long-Evans rats weighing 250-300g were purchased from Charles River Laboratories. All experiments were approved by the University of Washington Institutional Animal Care and Use Committee. Animals were group housed during initial acclimation and training sessions and were moved to single housing after surgery.

2.3.2 Reaching task.

After habituating to the facility and handlers for 1 week, rats were trained on a pellet reach task. Rats were placed into acrylic arenas that contained two vertical slots at the front of the arena in the left and right bottom corners. For initial determination of dominant forepaw, two plastic blocks with small divots were placed in front of each slot. Chocolate-flavored pellets were placed on each divot and the rat was guided to reach for the pellets by the experimenter. The amount of times rats successfully grabbed a pellet and pulled it back into the arena to eat it was tallied for each forelimb. Once the dominant forelimb was determined, rats moved onto the initial training phase.

During the initial training phase, one block corresponding with the dominant hand was placed in front of the corresponding arena slot. Rats were trained for 10 minutes at a time, once per day, 4-5 days per week. Scoring was determined based on five metrics: 1. Success – the rat successfully grabbed the pellet off the block, pulled it into the arena, and ate it; 2. Drop inside – the rat grabbed the pellet off the block, pulled it into the arena, but dropped it inside the arena before consuming it; 3. Drop outside – the rat grabbed the pellet off the block but dropped it before bringing it back into the arena; 4. Touch – the rat did not grab the pellet but did graze it with the dominant forepaw; and 5. Miss – the rat reached outside of the arena but did not make contact with the pellet. Scores were consolidated at the end of each week to determine each rat's proficiency in the task. Rats who

reached at least a 60% average success rate were scheduled for a spinal cord injury the following week.

2.3.3 ECoG array construction.

ECoG arrays were designed and constructed in the lab. Eight platinum-iridium tubes approximately 0.5mm in length and with an inner diameter of 0.56 mm (Johnson Mathey) were flattened and affixed in a 2 x 4 array using a flat adhesive. A nickel-titanium wire (Bioflex) was affixed to each tube and soldered to a 20 channel Hirose connector mounted on a printed circuit board. BioFlex wire was also soldered to the 12 remaining open channels on the board. Four Bioflex channels were used for grounds and references while the remaining 8 channels were grounded out.

2.3.4 Tetrode array construction.

Tetrode arrays were constructed in the lab following a protocol provided by the Hengen Laboratory at Washington University in St. Louis (Reikersdorfer et. al., 2021). For each tetrode, two strands of copper-coated wire (diameter 0.0012mm) were looped together and spun using a Tetrode Twister (OpenEphys). Spun wires were stripped using a solution of sulfuric acid before being soldered to a 20 channel Hirose board. Four tetrodes (totaling 16 channels) were affixed to each board. Four multi-stranded stainless steel wires, to create two grounds and two reference channels, were affixed to the remaining open channels. Tetrode tips were coated in a gold non-cyanide solution and impedance tested using a NanoZ device (White Matter LLC). Coating was reapplied until all impedances were between 0.1 and 0.3 MOhms.

2.3.5 Array implantation.

Rats were administered dexamethasone a day prior to surgery in order to reduce brain tissue swelling during implantation. Rats were anesthetized for surgery using isoflurane. An incision was made in the skin of the head to expose the skull. A craniotomy was performed over MCtx

(approximate coordinates 1.25AP/2.25ML) and the dura mater was removed. ECoG arrays were positioned on top of the brain tissue and fixed in place with GelFoam and a small amount of dental cement applied to the surrounding bone. Tetrode arrays were implanted at a depth of 1.5mm. Dental cement was used to cover the exposed skull and affix the Hirose connector in place. Rats were allowed to recover for a minimum of 1 week before beginning recordings.

2.3.6 Electrophysiological recordings.

Recordings were performed using either a custom wireless recording device constructed by the Electronics and Telecommunications Research Institute (ETRI), Daejeon, South Korea, or a Grapevine Neural Interface Processor (Ripple Neuro).

2.3.6.1 ETRI wireless recording device.

The ETRI wireless recording device was used to record ECoG signals only. The device used an ARM Core M4 floating point operation processor mounted on the device and transferred data wirelessly to a nearby computer using an enterprise service bus (ESB) system. The device was capable of recording from 16 unique channels but due to wireless data transfer constraints was only able to record and save data from 2 channels simultaneously with a sampling rate of 4096 Hz. Device setup and recording acquisition occurred on a custom MATLAB graphical user interface (GUI).

2.3.6.2 Ripple Neuro recording system.

The Grapevine Neural Interface Processor with the Nano2 front end (Ripple Neuro) was used to confirm ECoG data acquired using the ETRI wireless device and record from tetrode implants. The Ripple system with Nano2 front end was used to record up to 32 channels simultaneously at a sampling frequency of 30,000 Hz.

2.3.7 Sacrifice and tissue processing.

Rats were used for recordings for 4-6 months after implant. At the conclusion of the experiment, rats were deeply anesthetized using pentobarbital and transcardially perfused using 1X phosphate buffered saline (PBS) and a solution of 4% paraformaldehyde (PFA) in 1X PBS. The dental acrylic cap was removed and the position of the ECoG or tetrode array was determined.

2.3.8 Data analysis.

Data was analyzed using custom MATLAB (Mathworks) scripts and the Blackrock Neuro NPMK package (https://github.com/BlackrockNeurotech/NPMK).

2.3.7.1 ECoG analysis.

ECoG recordings acquired using the ETRI device were analyzed using custom MATLAB scripts. Recordings were bandpass filtered using a passband of 1 - 300 Hz and power spectra were determined using native MATLAB functions. ECoG recordings acquired using the Ripple Neuro system were analyzed using the Blackrock Neuro NPMK package and custom MATLAB scripts. Data was also bandpass filtered with a passband of 1 - 300 Hz.

2.3.7.2 Tetrode analysis.

Tetrode data was analyzed using the Blackrock Neuro NPMK package and custom MATLAB scripts. Individual data channels were sorted into corresponding tetrode groups and high-pass filtered with a lower limit of 300 Hz.

2.4 Results

2.4.1 ECoG array recordings

Custom ECoG arrays were constructed and implanted subdurally over the caudal forelimb area of MCtx after rats reached a minimum performance criteria in a pellet reach task (Fig. 1.1A). During initial testing, arrays were implanted in uninjured rats to ensure maximal motor activity for analysis. ECoG recordings were obtained while rats were performing the pellet reach task or ambulating around their arena (Fig. 1.2C). Recordings were analyzed offline and examined for overall noise level and whether there were clear indications of power changes indicative of movement.

Example traces and power spectra from one ECoG channel in one rat are shown in Fig. 1.3. Unfortunately, technical setbacks prevented clear analysis of recorded signals and determination of whether there was a sufficiently noise-free ECoG signal from which to trigger stimulation off of. The ETRI device (Fig. 1.3A) was limited by its recording of only two channels at a time, preventing analysis of all channels over the course of a recording session. Additionally, we had practical issues maintaining a secure connection between the device itself and the connector affixed on the rat, which likely contributed to issues with noise. Finally, although attempts were made to incorporate an infrared (IR) beam setup with the ETRI device in order to provide precise time points for each instance that the rat reached to grab a pellet, issues with recording from two devices at once prevented us from employing the IR beam effectively. As a result of these issues, we decided to try recording using a different acquisition system.

Given issues with the ETRI device, we attempted to record from the same arrays using the Ripple Neuro acquisition system (Fig. 1.3B). Unfortunately, we also ran into issues with noise that prevented clear delineation of signal fluctuations related to movement in the rat. The Ripple system is capable of recording at a much higher sampling frequency than the ETRI

device (30,000 Hz vs. 4096 Hz, respectively) but in turn seemed to pick up on new types of noise. Methods to prevent the noise during recording, such as use of a custom Faraday cage placed around the arena, and offline, such as filtering, did not seem to attenuate the noise. In addition, the Ripple system had its own set of practical difficulties that prevented its long-term use for TADSS therapy. The system does not have a commutator, necessitating untangling of the connecting cable periodically and preventing the type of extended recording sessions that are necessary for TADSS; rats undergoing TADSS therapy typically receive stimulation for 4-5 hours per day, whereas the maximum possible recording time on the Ripple with cable concerns was approximately 15 minutes. Additionally, the Ripple system is only capable of recording from four animals at once, which would have posed issues from an experimental throughput perspective.

Although there were significant issues with noise using both the ETRI device and Ripple system, there is some evidence that ECoG may be a useful trigger for TADSS eventually given the right conditions. Power spectra of recordings from both the ETRI and Ripple devices showed slight peaks that may correspond to an increase in power during movement. The ETRI device showed peaks around 75 and 90 Hz, and the Ripple device showed peaks at lower frequencies, around 10-20 Hz. There is some evidence that beta (~12-35 Hz) and gamma (50-100 Hz) band modulations occur during motor learning (Barone & Rossiter, 2021; Nowak & Stagg, 2018), providing some scant evidence that motor-related cortical oscillations can be picked up in the tested iterations of these recordings. However, given the noise in the signals and without a clear secondary indicator of movement initiation, it was difficult to interpret the power spectra as anything other than an intriguing anecdote.

Although it is somewhat promising that there's increased power in these bands, it is unclear why the peaks are different between different recording devices. Recordings were performed on different days, so it is possible that the rat's general movement around the arena and engagement in the task were different enough to support varied power in different bands. It

is also difficult to accurately interpret results from these recordings given the issues with noise and lack of an event indicator for volitional arm movements. Regardless, given the potential for a therapeutic, it is a question potentially worth pursuing in the future with a different acquisition system or potentially different arrays.

2.4.2 Tetrode recordings

In order to investigate changes in MCtx activity on the level of single units, tetrodes were constructed using a protocol provided by the Hengen laboratory (Washington University in St. Louis). Tetrodes were implanted around the same area of MCtx as ECoG arrays but lowered to a depth of 1.5mm in order to target activity from pyramidal cells in layer V. Tetrode recordings were acquired using the Ripple Neuro system described above.

Unfortunately, as with the ECoG recordings, noise in the acquired data prevented us from making any definitive conclusions about whether the tetrodes were effective in our hands at recording activity from single units in MCtx. Filtered, example traces from one tetrode array (four tetrodes, 16 channels total) are shown in Fig. 1.3A. Although tetrode groupings are relatively discernible from the traces, repetitive noise again prevented accurate filtering of the data and sorting of spikes.

Example traces from one tetrode (each channel in gray) and the average of those traces (in black) are shown in Fig. 1.3B. Although there are some fluctuations that visually appear as if they could be legitimate neuronal spikes, large noise deviations prevented sufficiently accurate analysis and sorting. One issue that became more obvious in the tetrode recordings (as opposed to the ECoG recordings) was the impact of rat movement and chewing on noise levels in the acquired data. Large epochs of noise were noted every time the rat moved too quickly (potentially jostling the headstage) or started chewing on a pellet. Unfortunately, given the nature of the pellet reach task, these noise deflections appear throughout most of the data and likely occur around the times that we would expect to see spiking activity in MCtx. A new

acquisition system obtained by the lab may help reduce some of these issues with noise although it has not been tested yet with these particular tetrodes.

2.5 Discussion

Unfortunately, we cannot draw any definitive conclusions from the ECoG or tetrode data acquired. Issues with noise in the data prevented us from definitively confirming that our arrays were picking up any type of neural signal and practical concerns about implementation of these devices for long-term, chronic recordings deterred us from pursuing these questions further.

Different acquisition systems may help determine whether we were able to record neural data from these implants. Previous members in the lab had difficulty acquiring clean signal from the Ripple system using commercially available arrays, and the ETRI device was used while in its development stages. Recent acquisition of a Tucker Davis Technologies system may provide future lab members with better neural recordings from both ECoG and tetrode arrays.

It is also quite possible that the ECoG and tetrode array designs were not adequate for collecting neural signals. In the data shown in Figure 1.2, the ECoG array was confirmed to be in the same location over MCtx as it was when implanted, but it is possible that a buildup of fluid or scar tissue beneath the array caused attenuation of neural signals. Additionally, other rats did have arrays that shifted over time. This could cause changes in neural signals recorded chronically, and if arrays shift out of contact with the brain tissue then it could cause an absence of signal altogether. It is unclear how many arrays we could expect to shift over time, and given the long time period of TADSS therapy it is necessary to determine better fixation of the arrays over the tissue before pursuing this as a chronic implant used for therapy.

It is also possible that the tetrode arrays were not adequate for recording single units, or that they shifted over time in a manner that was not picked up over the course of recording. Additionally, we first constructed the tetrodes to have 16 total channels as a first pass to see if they worked before scaling up to models with a larger number of channels. If different array

construction or acquisition systems show that these tetrodes are capable of detecting single units, we would have to determine a new design to increase the total number of channels in order to better tile cortical space and potentially get a view into population activity of MCtx ensembles before and after injury.

Unfortunately, due to the technical limitations, we did not learn anything about how MCtx activity changes after injury and with retraining alone or TADSS therapy. It will be interesting to see future experiments that are able to catalog this change and determine whether there are discernible differences depending on injury state and therapy level, and whether activity changes correlate with improvements in behavioral function.

Chapter 3

Assessment of virally-delivered transcription factors in improving axonal branching in SCI rats

3.1 Abstract

Spinal cord injuries (SCIs) cause significant damage to ascending and descending pathways to the spinal cord. Axonal regeneration of descending tracts is relatively limited and impairs the cord's capacity for functional recovery. Previous work has found that delivery of a combination of two transcription factors, KLF6 and NR25A (KN), significantly enhances corticospinal tract (CST) growth and branching after SCI. However, the increased branching does not translate to increased behavioral recovery. We hypothesized that directed plasticity of new CST branching using targeted, activity-dependent spinal stimulation (TADSS) would improve functional connectivity of new branches and overall improve functional outcomes. Unfortunately, technical limitations prevented us from confirming that the viral constructs carrying KN are effective in the rat. Whether KN can increase CST branching in the injured rat spinal cord and whether TADSS can help direct new connectivity remains unanswered.

3.2 Background

Spinal cord injuries (SCI) are typically the result of severed connections between descending pathways and their targets in the spinal cord (Ahuja et. al., 2017). Damaged axons following SCI do have some innate capacity for regrowth and plasticity following injury, allowing for some amount of spontaneous behavioral recovery (Raineteau & Schwab, 2001). However, the capacity for axonal regeneration after injury is limited and further curtailed by an inhospitable spinal microenvironment that includes factors such as glial scarring and molecules that repel axon growth (Guérout, 2021).

Currently investigated therapies for SCI typically fall into one of two categories. Some therapies try to take advantage of the innate plasticity of spared axons following injury. For example, TADSS aims to promote plasticity in spared circuits and strengthen connections in a behaviorally relevant motor loop. Other therapies attempt to increase the number of axons available to make connections, through methods such as introducing stem cells to the injured cord (Shinozaki et. al., 2021) or through delivery of transcription factors that promote axon growth (Venkatesh et. al., 2020).

Previous work in the Dr. Murray Blackmore's lab at Marquette University found that KLF6 and NR25A, two transcription factors, were in combination able to significantly increase the growth of spared CST axons following a spinal cord injury in mice. Although this KN construct greatly increased CST axon regeneration, the increase in descending fibers did not translate into improved behavioral recovery in the injured animals. One hypothesis regarding this discrepancy is that increased axonal output without behaviorally relevant, guided plasticity fails to create meaningful connections between new descending axons and preserved targets in the spinal cord (Kramer et. al., 2021).

We hypothesized that administration of the KN transcription factors combined with targeted, activity-dependent spinal stimulation (TADSS) would improve behavioral outcomes in an injured rat model over administration of KN or TADSS alone. Specifically, we hypothesized that the activity-dependent stimulation hallmark of TADSS would help guide new CST branches to form functionally relevant connections that could improve overall behavioral recovery.

To test this hypothesis, we first examined whether the KN viral construct would promote CST axon regeneration in the rat and assess how its delivery impacted recovery after injury with retraining alone. Dr. Blackmore has not studied the effect of KN therapy in rats. Unfortunately, technical difficulties prevented us from getting a clear answer as to whether the virus construct works in the rat to increase axonal regrowth of CST axons. The project is ongoing, with initial results expected in 2024.

3.3 Methods

Animals.

Long-Evans rats weighing 250-300g were purchased from Charles River Laboratories. All experiments were approved by the University of Washington Institutional Animal Care and Use Committee.

Viruses.

All viruses were prepared by the Blackmore Lab at Marquette University. All rats were injected with AAV9-mScarlet in MCtx. Rats were divided into two groups and injected with either retroAAV2-KN-GFP or retroAAV2-GFP in the spinal cord.

Reaching task.

Initial training on a pellet reach task was performed as described in Chapter 2.

Spinal cord injury.

Rats were anesthetized with a combination of ketamine and xylazine. The dorsal musculature was retracted and a hemilaminectomy was made at the C4 vertebrae. After exposure of the spinal cord, rats were fitted into an Ohio State impact device and received a controlled impact onto one side of the spinal cord at C4, corresponding with the rat's dominant forelimb. Musculature and skin were closed and rats received a postoperative course of buprenorphine for pain management and enrofloxacin for infection prevention. Rats were monitored twice daily for the week following injury. Bladder expression was performed twice daily until bladder function returned (typically 1-2 days post-injury) and weights were monitored daily. Rats were allowed to recover for 4-6 weeks post-injury without further training or surgeries.

Viral injections.

Viral injections were performed 8 weeks after SCI. All rats received an injection of anterograde AAV9-mScarlet at two sites in MCtx (approximate coordinates 1.5AP/2.5ML/-2.0DV and 1.0AP/2.0ML/-2.0DV). 1000nL of virus was injected at each cortical site. The cortical virus contained only fluorescent markers and no transcription factors, in order to visualize the descending corticospinal tract in the spinal cord. Rats were randomized into two groups for the spinal injections: one group received an injection of retroAAV2-KN-GFP, which contained the KN transcription factors and the other which received a control injection of retroAAV2-GFP which contained only a fluorescent indicator. Experimenters were blinded to virus identity. Spinal viruses were delivered at two depths (-0.5 and -1.0DV) at the C5 level of the spinal cord, with 1000nL of virus delivered at each depth. Rats were allowed to recover for 6 weeks before starting retraining.

A secondary test round was performed using only the retroAAV2-GFP virus and no cortical virus.

Retraining.

The rats' baseline reaching performance following injury and viral injections was assessed. In addition to the scoring criteria described in Chapter 2, post-injury rats were also scored on attempts, wherein they tried to raise their injured forelimb up to the slot. After assessing baseline, rats resumed retraining, 10 minutes per day, 4-5 times per week for 8 weeks.

Tissue processing.

Following 8 weeks of retraining, rats were deeply anesthetized with 1cc pentobarbital and transcardially perfused using 1X phosphate buffered saline (PBS) and a solution of 4% paraformaldehyde (PFA) in 1X PBS. Brain and spinal cord tissue was extracted and post-fixed overnight in 4% PFA. TIssue was transferred to 1X PBS and kept refrigerated at 4C until being sent

to Marquette University for processing. Samples were sectioned on a vibratome, mounted, and imaged using a confocal microscope.

A secondary round of test imaging was done in-house at UW. Animals were anesthetized and perfused as described above. Brains and spinal cords were post-fixed overnight in 4% PFA and transferred to a 20% sucrose solution in 1X PBS for at least 24 hours. Tissue was embedded in Tissue-Tek OCT compound and sliced into 30um coronal sections on a cryostat. Slides were prepared with DAPI counterstain. Slides were imaged on a Leica widefield microscope at the Keck Microscopy Center (University of Washington). Images were analyzed using Leica's LAS X viewer.

3.4 Results

18 rats were tested over the course of six months. Rats were trained on a pellet reach task until reaching a minimum average percent success criteria, typically taking 3-4 weeks, before receiving a contusion spinal cord injury at cervical level 4. In order to more closely replicate a chronic injury state in the spinal cord and to prevent virus uptake by immune cells in the immediate wake of injury (Ahuja et. al., 2017), rats were allowed to recover for 8 weeks before viral injection (Fig. 4A). Each rat was injected with a red fluorescent AAV9-mScarlet virus in the cortex in order to visualize CST-specific projections to the spinal cord. Rats were randomly assigned one of two green fluorescent retrograde viruses that were injected into the spine: a GFP-only control virus or a GFP virus that contained the KN construct (Fig. 4B,C). Pellet task retraining resumed 6 weeks after injection to allow animals time to recover and to ensure adequate viral expression. Rats retrained on the pellet task for 8 weeks before tissue was extracted and sent for processing (Fig. 4A).

Based on previous work with these viruses (Venkatesh et. al., 2020), we expected to see non-CST cortical cells labeled with red in cortex, non-CST spinal cells labeled in green in the spinal cord, and yellow co-labeled putative CST neurons in cortex and spinal cord. Unfortunately, viral expression for the cortical virus and both spinal viruses were extremely inconsistent between animals. A representative example of expression patterns in MCtx and the spinal cord is shown in Fig. 5A. A number of rats showed almost no expression of either virus (Fig. 5A.1), while others

showed sparse expression of one or both viruses (Fig. 5A.2). Although some rats did have decent viral expression of both viruses in both MCtx and spinal cord, there were no rats with significant co-labeling of putative CST neurons (Fig. 5A.4). It is also unclear why there is GFP labeling in layers other than layer V of cortex. Descending CST projection neurons to the spinal cord originate in layer V and are the only known cortical neurons to project directly to the spinal cord, so virus taken up by the terminals of these neurons in the cord should show GFP labeling only in layer V. Additionally, although we injected the spinal viruses only on one side of the spinal cord, we see bilateral GFP labeling of cortex in several samples.

Additionally, although the cortical virus in some instances showed good expression in descending fibers (panels 3 and 4), neither spinal virus showed clear fiber expression. This is surprising considering there were several samples showing spinal virus expression in the cortex, suggesting that the virus was taken up by axon terminals in the cord.

Expression levels of all viruses were quantified on a scale of 0 to 3, with 0 being no visible expression and 3 being the densest amount of expression seen in these samples (Fig. 5B). Expression levels varied greatly between rats but there was no significant difference seen in mean expression levels between rats that received the KN spinal virus and rats that received the control spinal virus.

Comparison of pellet retraining scores between rats that received the KN virus and rats that received the control virus showed no evident difference (Fig. 6). This result is unsurprising both because of the sporadic expression patterns of the viruses in both groups and because, even if the viruses had successfully promoted CST arborization, introduction of KN was shown to have no effect on behavioral recovery in mice (Kramer et. al., 2021).

Viruses were retested at different volumes to see the minimum possible volume required for transmission to contralesional MCtx without significant spillover to ipsilesional cortex (Fig. 7). These tests confirmed that the retrograde GFP virus did indeed travel as far as MCtx consistently. However, expression is rather weak and seems to be concentrated in the soma, which does raise concerns

about the efficacy of these viruses in the rat for assessing changes in more distal processes such as axon terminals and dendrites.

3.5 Discussion

We were unable to produce conclusive results about the efficacy of these viruses in a rat model or determine whether the KN construct induces axonal branching in the rat in a similar fashion to that seen in mice. It is likely that experimenter error caused the sporadic viral expression patterns. One possibility is that the virus injections in cortex overshot the desired coordinates and landed in the ventricles instead, spreading virus out from the intended target of layer V in MCtx. Unfortunately, since these samples were processed off-site, we are unable to independently access images of other brain areas to confirm total virus spread in each animal.

Another possible source of experimenter error is syringe and injector use. In early injections one syringe was used for all viruses, and although the syringe was cleaned and soaked in ethanol between viruses it is highly possible that our cleaning method was not sufficient and caused cross contamination of virus types. This was rectified in later injections with the addition of separate syringes for all three viruses. Additionally, it is possible that unnoticed issues with clogging of the injection syringe prevented injections of full virus volume in some rats, which could explain why expression density varies so widely between animals. A higher than necessary viral injection volume could also explain the bilateral GFP labeling of cortex in some samples. It is possible that the virus injected unilaterally in the cord diffused enough to infect terminals on both sides of the cord, thereby bilaterally labeling cortex.

It is possible that the viruses themselves are not as effective in the rat as in the mouse. Although other studies have shown that retro-AAV efficiently transduces cortical cells descending to the spinal cord (Metcalf et. al., 2022), this was the first test of these specific constructs in the rat. Unfortunately we do not have access to titer concentration or the full construct of this specific batch of viruses to compare with previously reported concentrations and constructs used in the rat.

Although the initial virus test did not produce convincing evidence that the viruses expressed well in the rats, later tests with varied retrograde virus volume did at least seem to transport to MCtx and putative CST neurons more consistently. It is still not clear why fluorescent protein expression of these viruses is punctate and seemingly restricted to the soma rather than cell-filling as is seen with similar viral constructs. These samples were not stained with antibodies that could amplify the signal, so it is possible that processes do contain fluorescent protein that would be detectable with further amplification.

Currently this projection is in its next phase, where injured rats are injected with either the KN or control virus and put through TADSS therapy. We hypothesize that the TADSS therapy will guide new CST sprouting caused by the KN virus, and hopefully improve behavioral outcomes better than TADSS therapy alone. Work is ongoing with initial results expected in 2024.

Chapter 4

Conclusions and future directions

4.1 Conclusions and future directions of described projects.

Unfortunately, this work provides no solid conclusions on the mechanism of TADSS therapy and whether it is mediated at least in part by the CST. We can conclude that improved recording devices and analysis and further interrogation of the viruses used may still shed some insights on the nature of TADSS. The viral tracing project is ongoing, with first results expected in early 2024, and should illuminate whether delivery of transcription factors like KN combined with TADSS therapy improves behavioral outcomes after injury better than TADSS therapy or KN expression alone.

Although it is difficult to propose future directions for experiments that did not work, it is interesting to think about what might have been. We hypothesize that TADSS is mainly exerting its effects through plastic changes in the CST due to the pathway's unique role in forelimb fine motor control. However, prior work has shown that other descending pathways, such as the reticulospinal tract, play an important role in fine motor skill recovery after injury (Asboth et. al., 2018, Engmann et. al., 2020). TADSS stimulation is nonspecific and is likely activating numerous cell types over a wide area. It is possible that the behavioral improvements seen after TADSS therapy are due to improved connections in other descending pathways, although whether those connections are more or less critical to behavioral recovery than the CST remains unclear. Additionally, TADSS could be mediating connections between preserved ascending sensory pathways, which are relatively unexplored but seem to play an important role in recovery as well (Takeoka & Arber, 2019). Future experiments examining anatomical changes in MCtx, but also in nuclei of other descending and ascending spinal pathways, such as the cerebellum, pons, reticular nucleus, and striatum, could shed some interesting results on the scope of TADSS' effect on preserved pathways.

Similarly, it is unclear whether TADSS combined with increased axonal sprouting in the CST through transcription factors like KN helps improve behavioral recovery. It is also possible that delivering KN to other descending or ascending pathways in the spinal cord could improve sprouting of preserved neurons as well as it does in the CST.

4.2 Other investigations into TADSS.

One interesting thread of investigation that I began but has not progressed sufficiently to be included in this thesis involves examination on the effects of TADSS combined with multiple trained behaviors. Rats can be trained on multiple behavioral tasks that all utilize forelimb movements other than the pellet reach task described above. Previous work in the lab hypothesized that retraining rats on multiple tasks during TADSS therapy would help generalize recovery and perhaps improve overall functioning or improve functioning on a faster timescale than that seen with one task alone. However, preliminary data found that stimulating during one task actually seemed to interfere with recovery in related tasks, with rats regaining considerable function in the stimulated task and performing significantly worse than their counterparts on the unstimulated task. Although these results are intriguing, the low number of rats tested requires further experiments before concluding that TADSS stimulation on one task interferes with recovery in similar but distinct tasks. The first group of rats are currently finishing initial training and initial results are expected by mid-2024.

Overall, although the experiments described above did not produce any conclusive results or evidence of the mechanism behind TADSS, they did reveal some technical deficiencies that have been corrected for future experimenters. Hopefully in the near future we will gain a better understanding of how TADSS is mediating improved functional recovery in the rat and start to determine how this therapy can be implemented in human patients living with SCIs.

Appendix A: Figures

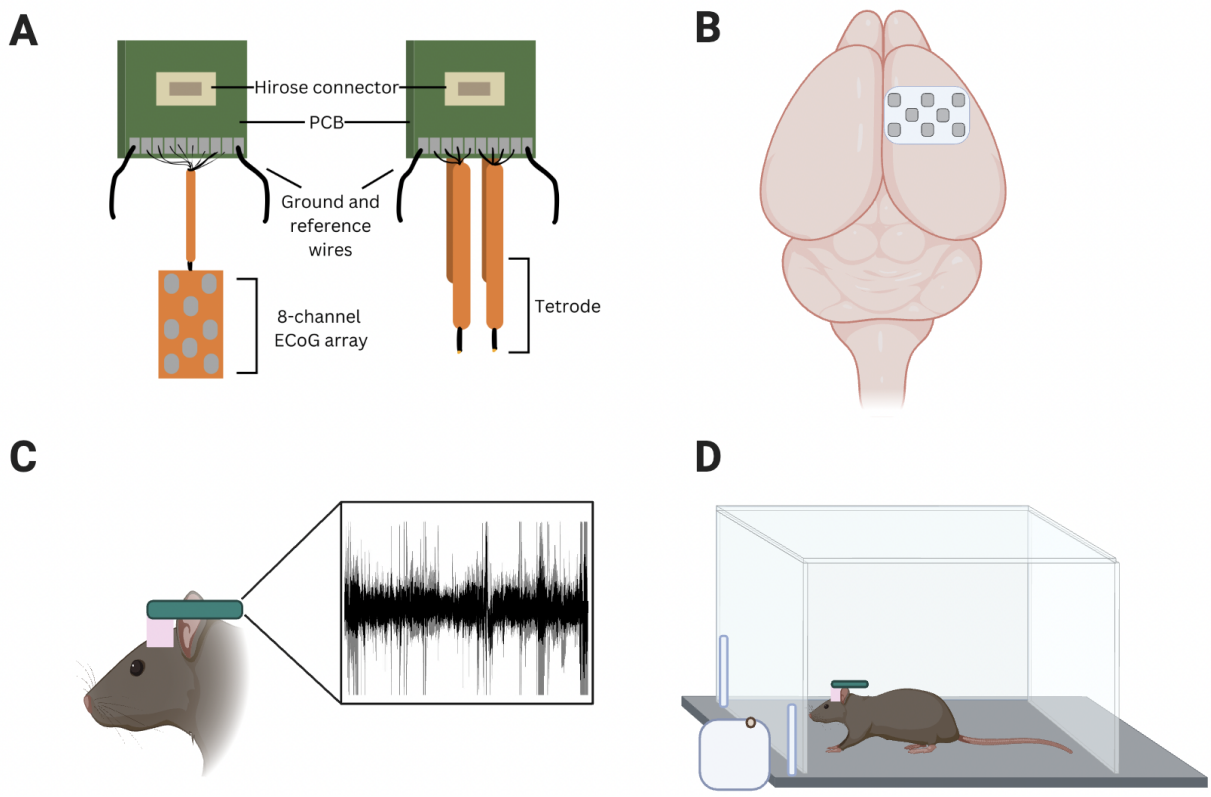

Figure 1: Electrophysiological arrays and recording setup.

(A) Array setup. ECoG arrays were constructed of 8 small discs arranged approximately 1mm apart, while tetrodes consisted of 4 4-wire bundles. All arrays were soldered to a PCB board housing a Hirose connector. **(B)** Approximate location of array implantation. ECoG arrays were implanted subdurally over the caudal forelimb area of motor cortex while tetrode arrays were implanted to a depth of -1.5mm. **(C,D)** After recovery from surgery, rats were placed in an acrylic arena and prompted to do a pellet reach task while recordings were carried out. Wireless recordings with the ETRI device allowed rats to move freely around the arena, while tethered recordings with the Ripple or Neurochip somewhat limited animal movement. Recording periods typically lasted from 1 to 5 minutes, with up to 10 recording sessions per day.

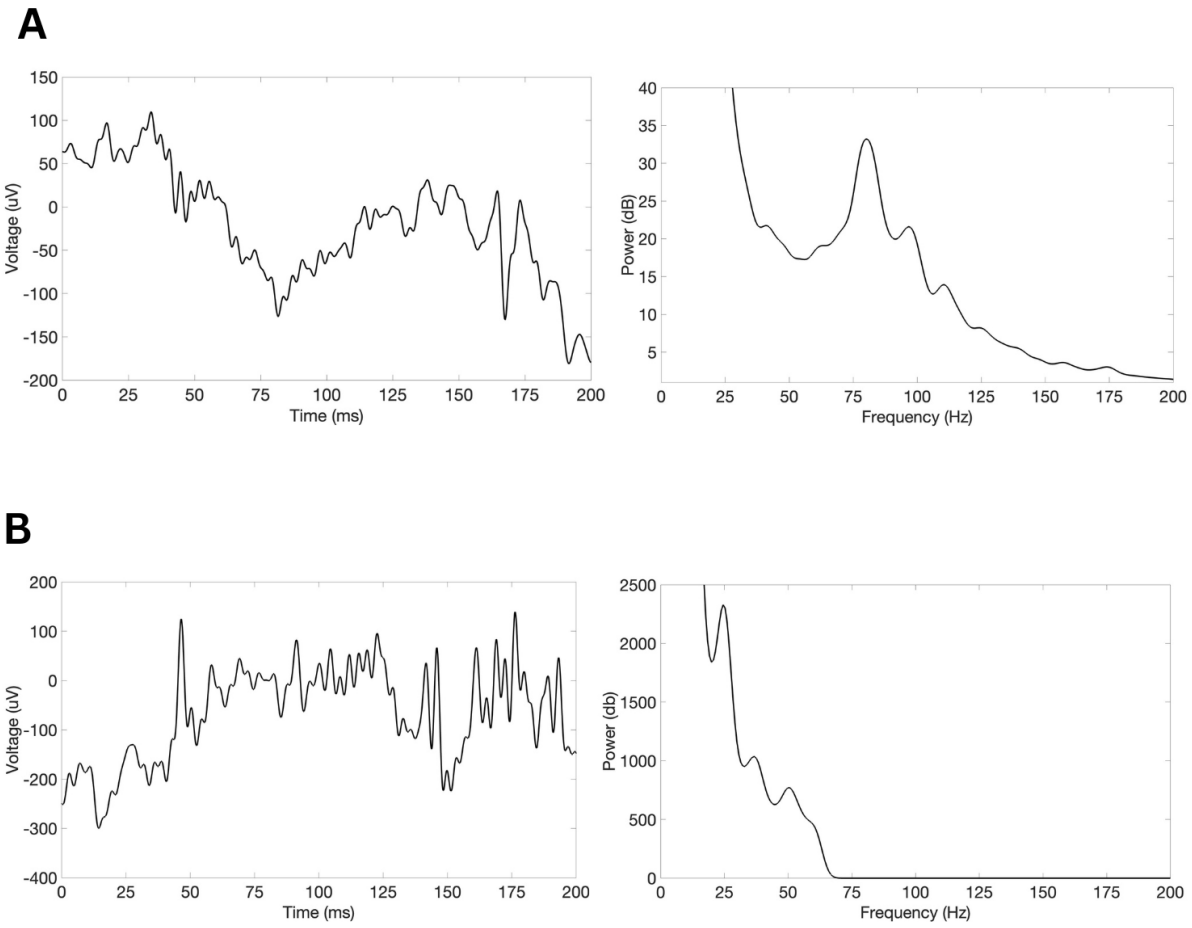

Figure 2: Example ECoG data.

Example recordings from one rat implanted with an ECoG array. Recordings were taken using two different acquisition systems. **(A)** Representative recording from one channel (left) using the ETRI acquisition system. Data was bandpass filtered from 1-300 Hz. Corresponding spectral density is displayed at right. Slight peaks were seen around 75 Hz and 90Hz. **(B)** Representative recording from one channel using the Ripple Neuro acquisition system. Data was bandpass filtered from 1-300 Hz. Corresponding spectral density is displayed at right. Slight peaks were seen around 25 Hz and 50 Hz. Noisy samples and inconsistent results from week to

week and between recording systems prevented us from consistently determining an appropriate ECoG signal to use as a trigger for TADSS stimulation.

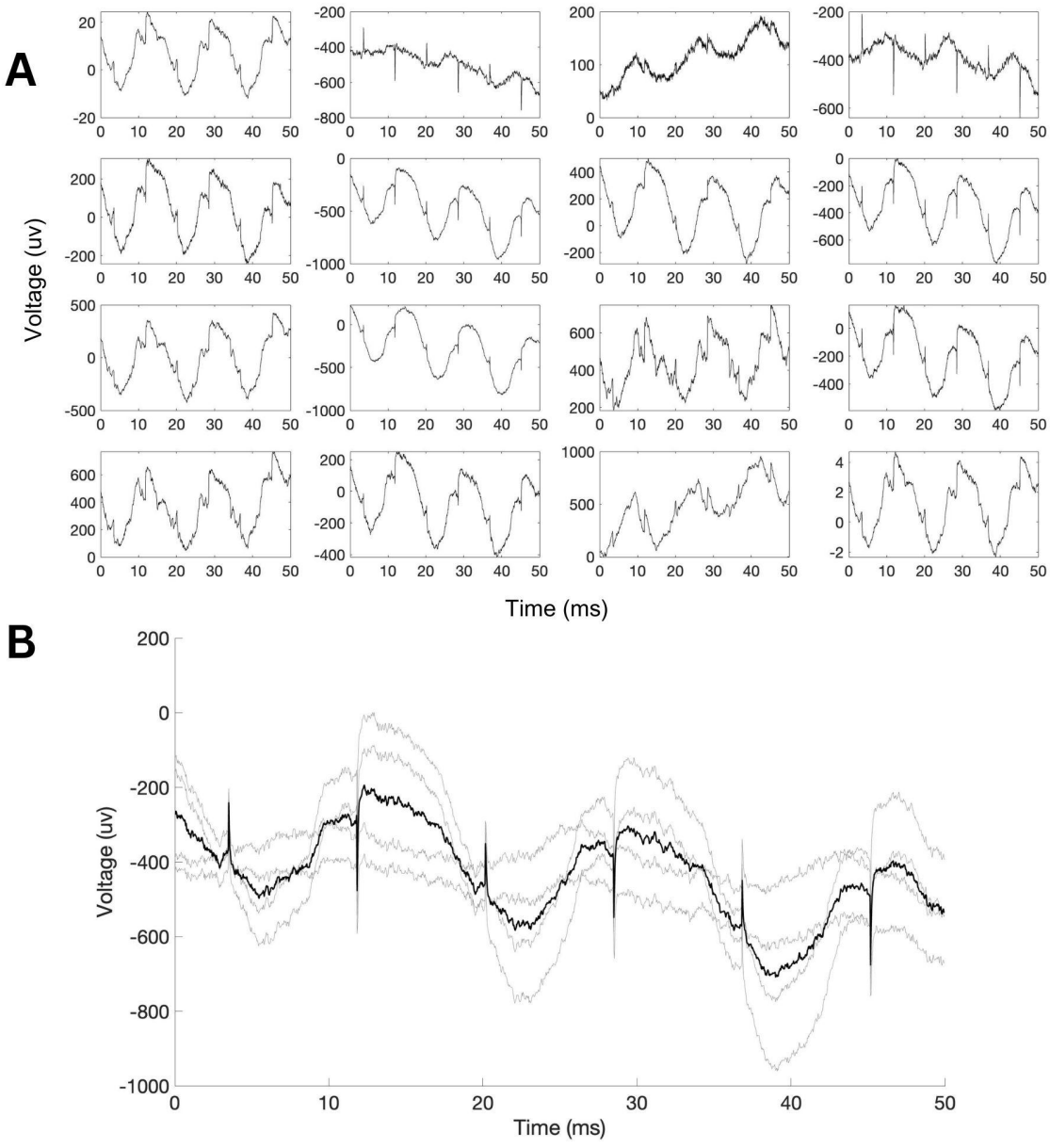

Figure 3: Example tetrode data.

Example tetrode recordings from one rat implanted with a 16-channel (4-tetrode) array. **(A)** Representative data from one tetrode array (four tetrodes, 16 channels total). A high-pass filter (300 Hz) was applied to all recordings. There is some visual evidence of similarity between

channels on each tetrode, but repetitive noise in every channel prevented clear evidence of spikes. **(B)** Example recording from one tetrode. Gray traces show recording from each channel in one tetrode, black trace is the average of all four channels. Although there are some waveforms that visually appear as if they could be spikes, large deflections, presumably noise, throughout the sample prevented accurate sorting of potential spike waveforms.

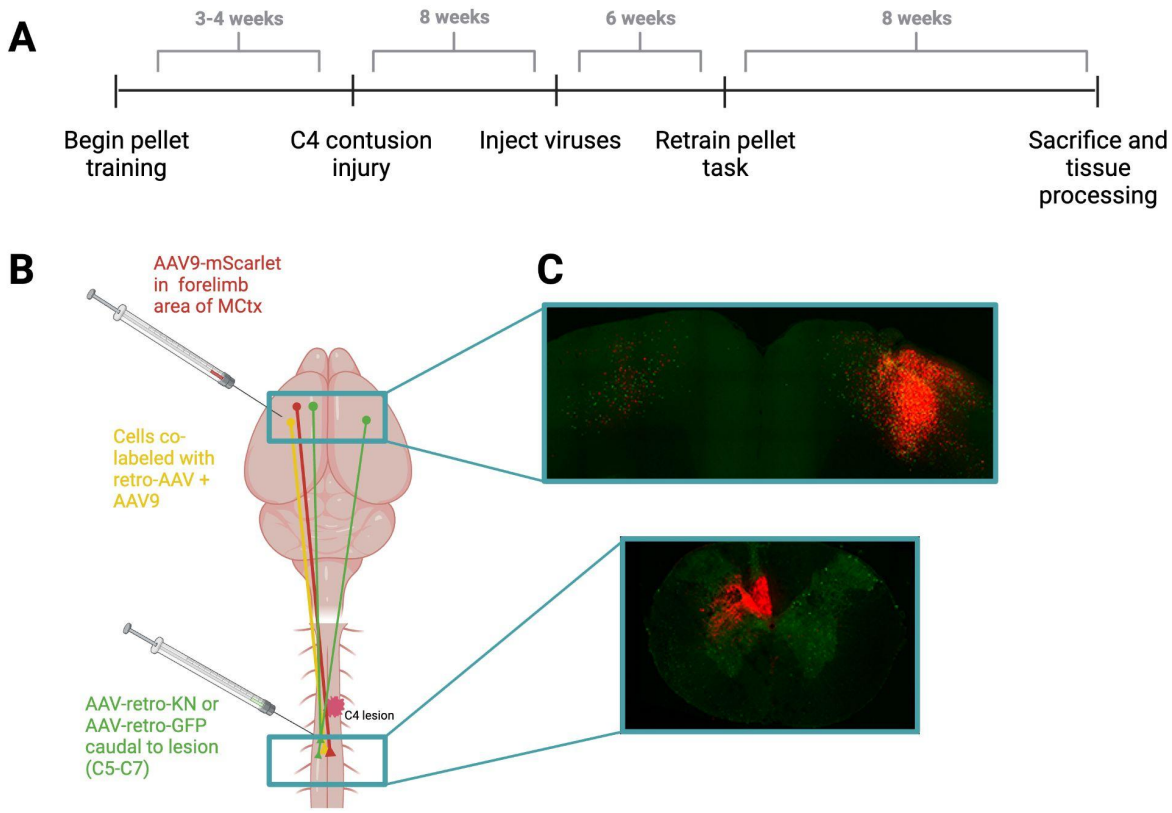

Figure 4: Viral strategy and experimental design.

(A) Rats were initially trained in a pellet reach task until reaching a threshold of >60% average success rate per week of training. After injury, rats received an injection of AAV9-mScarlet in MCtx and either rAAV2-retro-KN or rAAV2-retro-GFP in the spinal cord **(B, C)**. Rats were randomly assigned to the experimental or control group and experimenters were blinded to virus identity. After a recovery period rats were retrained on the pellet reach task for 8 weeks before tissue was

extracted and sent for processing. **(C)** Example images of brain (top) and spinal cord (bottom) from a rat injected with AAV9-mCherry in cortex (red) and AAV-retro-KN in spinal cord (green).

A

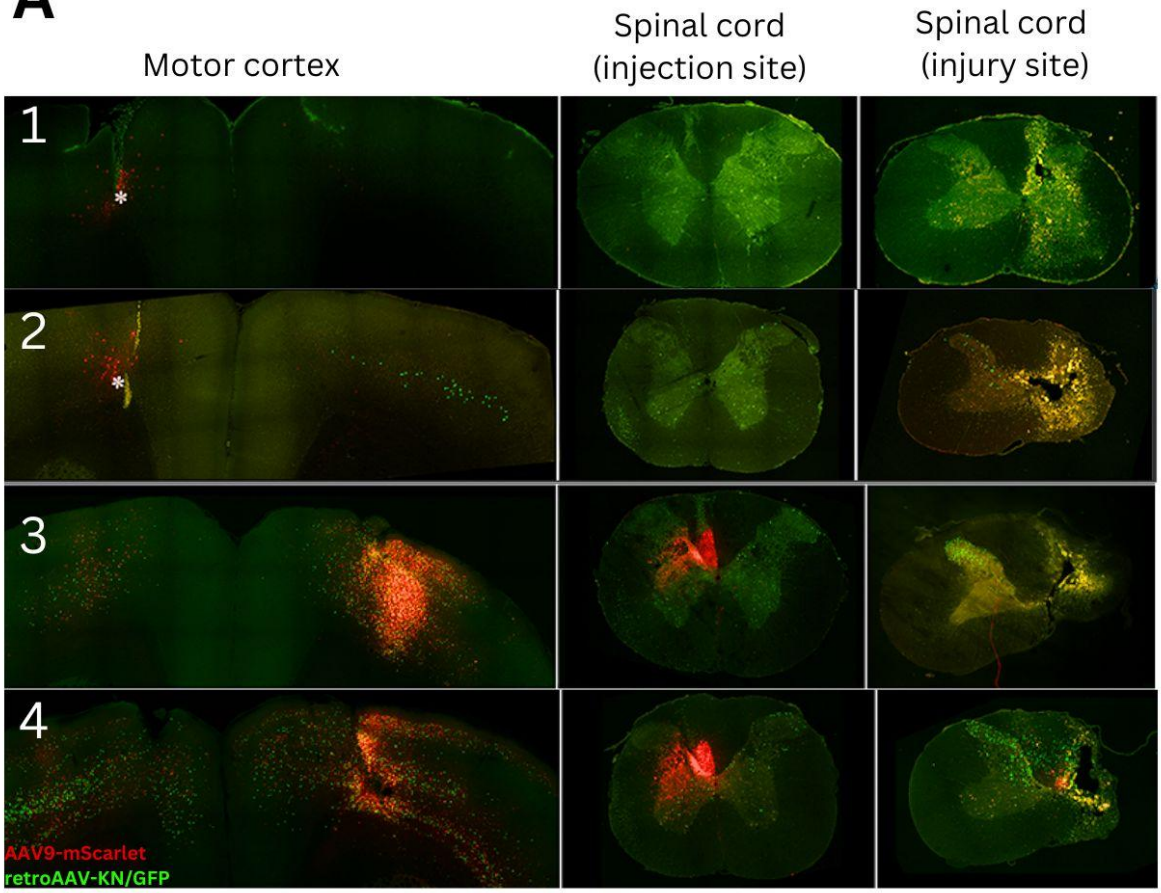
Motor cortex
Spinal cord (injection site)
Spinal cord (injury site)
1
2
3
4
AAV9-mScarlet
retroAAV-KN/GFP

B

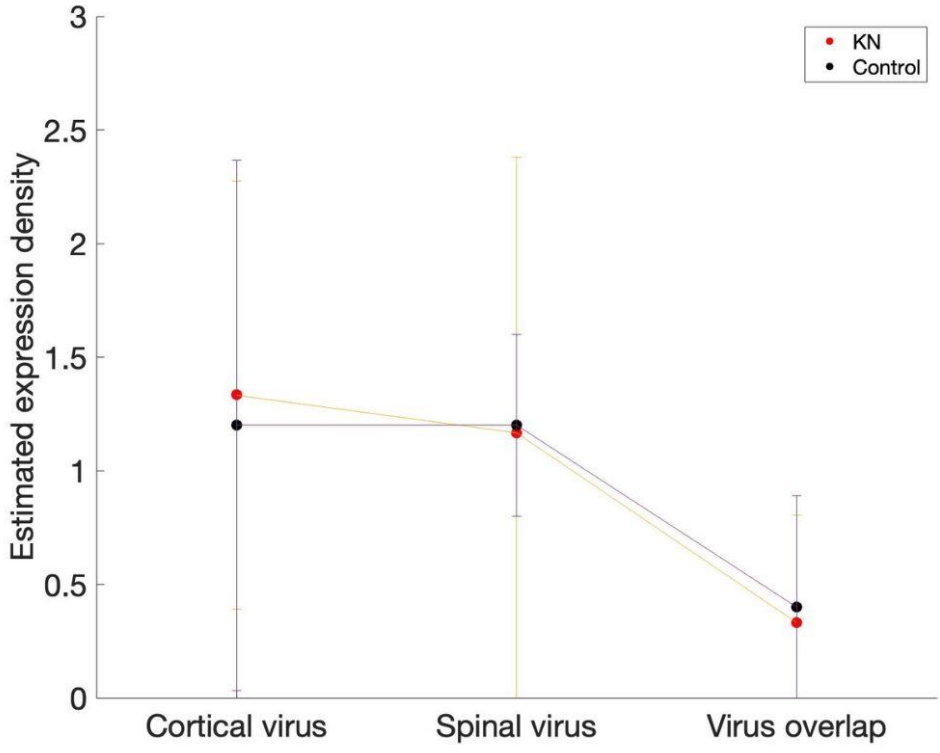
KN
Control
Estimated expression density
3
2.5
2
1.5
1
0.5
0
Cortical virus
Spinal virus
Virus overlap

Figure 5: Initial virus test showed inconsistent expression of all three viruses.

Representative range of viral expression patterns are shown in **(A)**. Left panels show expression around approximate cortical virus (AAV9-mScarlet) injection epicenter in MCtx, middle panels show approximate spinal virus (retro-AAV-KN-GFP or retro-AAV-GFP) injection epicenter area in the spinal cord, right panels show approximate epicenter of C4 contusion injury. Expression of all three viruses varied widely in location and density between rats. Expression density was quantified on a scale of 0-3, with 0 being no expression and 3 being dense expression. Mean expression density and standard deviation are shown in **(B)**. Red indicates rats that received the KN spinal virus; black indicates rats that received the control spinal virus; all rats received the same cortical virus. Mean viral expression and overlap between the cortical and spinal viruses did not differ between the control and KN groups.

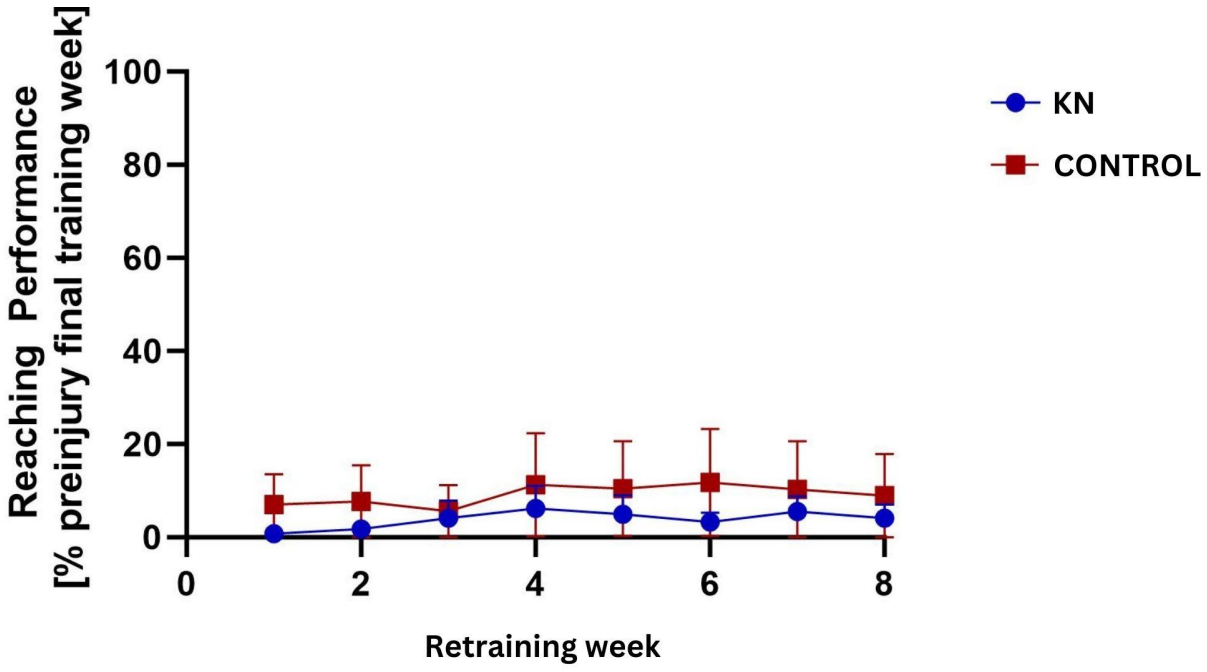

Figure 6: Rat reaching performance does not change based on virus type injected.

Rats in both the KN virus (red) and control virus (blue) groups had similarly low reaching performance after injury and virus injections. Reaching performance is expressed as the average percentage of successful pellet grabs per injury retraining week divided by the average percentage of successful pellet grabs per final week of initial training period. Given prior results in the Blackmore lab and due to the sporadic nature of viral expression in these rats, it is unsurprising that the KN virus had no clear effect on behavioral recovery after injury.

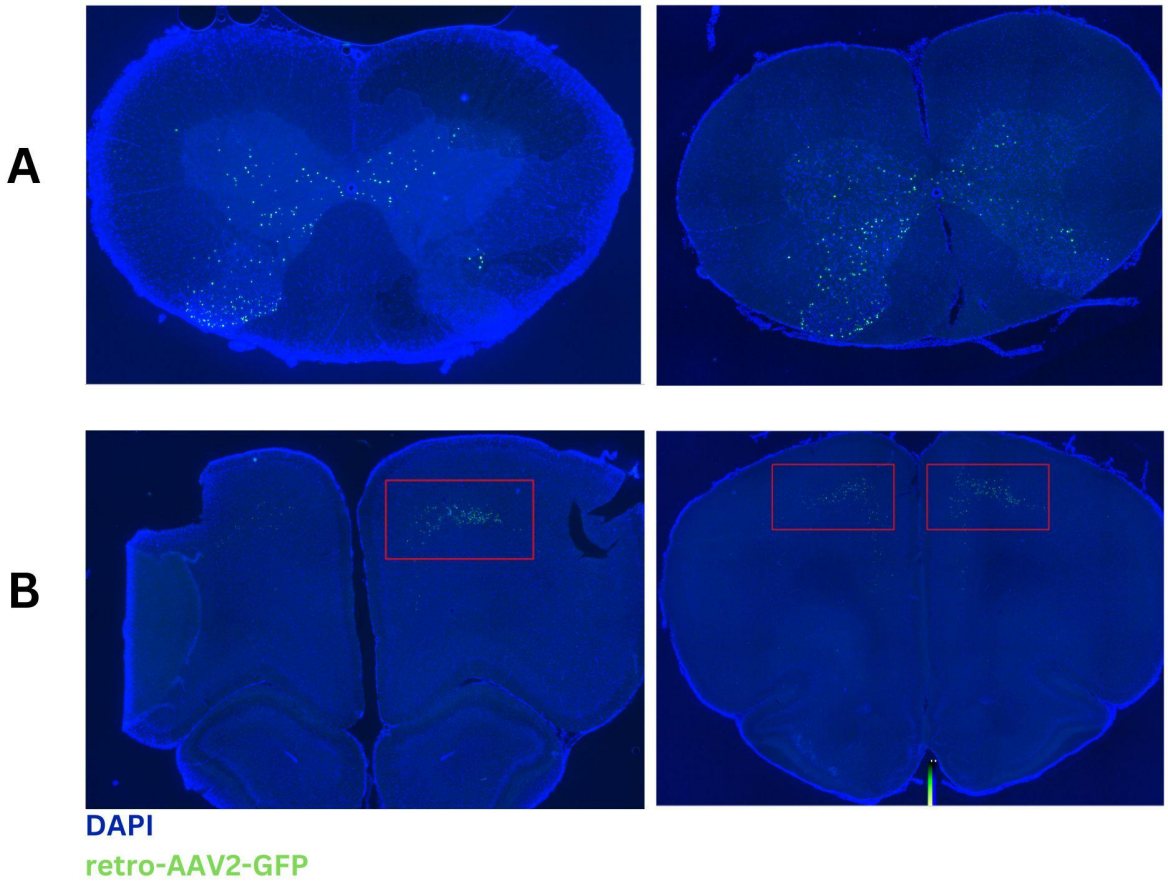

Figure 7: Retesting virus volumes showed more consistent expression in spinal cord and motor cortex.

Retesting the retrograde viruses at higher volumes showed more consistent expression in **(A)** spinal cord and **(B)** motor cortex. Higher volumes (right panels) injected into the spinal cord appear to leak

past the midline and cause GFP expression in both hemispheres **(B, bottom right)**. Punctate expression patterns in both spinal cord and MCtx suggest that GFP does not traffic into more distal dendrites or axon endings, creating a potential issue for determining differences in axonal arborization with the KN and GFP viruses.

Appendix B: Bibliography

1. Ahuja, C. S., Wilson, J. R., Nori, S., Kotter, M. R. N., Druschel, C., Curt, A., & Fehlings, M. G. (2017). Traumatic spinal cord injury. Nature Reviews Disease Primers, 3(1), 17018. https://doi.org/10.1038/nrdp.2017.18
2. Anderson, M. A., Squair, J. W., Gautier, M., Hutson, T. H., Kathe, C., Barraud, Q., Bloch, J., & Courtine, G. (2022). Natural and targeted circuit reorganization after spinal cord injury. Nature Neuroscience, 25(12), 1584–1596. https://doi.org/10.1038/s41593-022-01196-1
3. Asboth, L., Friedli, L., Beauparlant, J., Martinez-Gonzalez, C., Anil, S., Rey, E., Baud, L., Pidpruzhnykova, G., Anderson, M. A., Shkorbatova, P., Batti, L., Pagès, S., Kreider, J., Schneider, B. L., Barraud, Q., & Courtine, G. (2018). Cortico–reticulo–spinal circuit reorganization enables functional recovery after severe spinal cord contusion. Nature Neuroscience, 21(4), 576–588. https://doi.org/10.1038/s41593-018-0093-5
4. Barbiellini Amidei, C., Salmaso, L., Bellio, S., & Saia, M. (2022). Epidemiology of traumatic spinal cord injury: A large population-based study. Spinal Cord, 60(9), 812–819. https://doi.org/10.1038/s41393-022-00795-w
5. Barone, J., & Rossiter, H. E. (2021). Understanding the Role of Sensorimotor Beta Oscillations. *Frontiers in Systems Neuroscience*, *15*, 655886. https://doi.org/10.3389/fnsys.2021.655886
6. Bi, G., & Poo, M. (1998). Synaptic Modifications in Cultured Hippocampal Neurons: Dependence on Spike Timing, Synaptic Strength, and Postsynaptic Cell Type. The Journal of Neuroscience, 18(24), 10464–10472. https://doi.org/10.1523/JNEUROSCI.18-24-10464.1998
7. Engmann, A. K., Bizzozzero, F., Schneider, M. P., Pfyffer, D., Imobersteg, S., Schneider, R., Hofer, A.-S., Wieckhorst, M., & Schwab, M. E. (2020). The Gigantocellular Reticular Nucleus Plays a Significant Role in Locomotor Recovery after Incomplete Spinal Cord Injury. *The Journal of Neuroscience*, *40*(43), 8292–8305. https://doi.org/10.1523/JNEUROSCI.0474-20.2020
8. Gómara-Toldrà, N., Sliwinski, M., & Dijkers, M. P. (2014). Physical therapy after spinal cord injury: A systematic review of treatments focused on participation. *The Journal of Spinal Cord Medicine*, *37*(4), 371–379. https://doi.org/10.1179/2045772314Y.0000000194
9. Guérout, N. (2021). Plasticity of the Injured Spinal Cord. *Cells*, *10*(8), 1886. https://doi.org/10.3390/cells10081886
10. Hachem, L. D., Ahuja, C. S., & Fehlings, M. G. (2017). Assessment and management of acute spinal cord injury: From point of injury to rehabilitation. *The Journal of Spinal Cord Medicine*, *40*(6), 665–675. https://doi.org/10.1080/10790268.2017.1329076
11. Hu, X., Xu, W., Ren, Y., Wang, Z., He, X., Huang, R., Ma, B., Zhao, J., Zhu, R., & Cheng, L. (2023). Spinal cord injury: Molecular mechanisms and therapeutic interventions.

Signal Transduction and Targeted Therapy, 8(1), 245. https://doi.org/10.1038/s41392-023-01477-6
12. Kramer, A. A., Olson, G. M., Chakraborty, A., & Blackmore, M. G. (2021). Promotion of corticospinal tract growth by KLF6 requires an injury stimulus and occurs within four weeks of treatment. *Experimental Neurology*, *339*, 113644. https://doi.org/10.1016/j.expneurol.2021.113644
13. Lemon, R. N. (2008). Descending Pathways in Motor Control. *Annual Review of Neuroscience*, *31*(1), 195–218. https://doi.org/10.1146/annurev.neuro.31.060407.125547
14. Marquez-Chin, C., & Popovic, M. R. (2020). Functional electrical stimulation therapy for restoration of motor function after spinal cord injury and stroke: A review. BioMedical Engineering OnLine, 19(1), 34. https://doi.org/10.1186/s12938-020-00773-4
15. McPherson, J. G., Miller, R. R., & Perlmutter, S. I. (2015). Targeted, activity-dependent spinal stimulation produces long-lasting motor recovery in chronic cervical spinal cord injury. Proceedings of the National Academy of Sciences, 112(39), 12193–12198. https://doi.org/10.1073/pnas.1505383112
16. Metcalfe, M., Yee, K. M., Luo, J., Martin-Thompson, J. H., Gandhi, S. P., & Steward, O. (2022). Harnessing rAAV-retro for gene manipulations in multiple pathways that are interrupted after spinal cord injury. *Experimental Neurology*, *350*, 113965. https://doi.org/10.1016/j.expneurol.2021.113965
17. National Spinal Cord Injury Statistical Center, Traumatic Spinal Cord Injury Facts and Figures at a Glance. Birmingham, AL: University of Alabama at Birmingham, 2023. https://www.nscisc.uab.edu/public/Facts%20and%20Figures%202023%20-%20Final.pdf
18. Nishimura, Y., & Isa, T. (2012). Cortical and subcortical compensatory mechanisms after spinal cord injury in monkeys. Experimental Neurology, 235(1), 152–161. https://doi.org/10.1016/j.expneurol.2011.08.013
19. Noreau, L., Noonan, V., Cobb, J., Leblond, J., & Dumont, F. (2014). Spinal Cord Injury Community Survey: A National, Comprehensive Study to Portray the Lives of Canadians with Spinal Cord Injury. Topics in Spinal Cord Injury Rehabilitation, 20(4), 249–264. https://doi.org/10.1310/sci2004-249
20. Nowak, M., Zich, C., & Stagg, C. J. (2018). Motor Cortical Gamma Oscillations: What Have We Learnt and Where Are We Headed? *Current Behavioral Neuroscience Reports*, *5*(2), 136–142. https://doi.org/10.1007/s40473-018-0151-z
21. Raineteau, O., & Schwab, M. E. (2001). Plasticity of motor systems after incomplete spinal cord injury. Nature Reviews Neuroscience, 2(4), 263–273. https://doi.org/10.1038/35067570
22. Reikersdorfer, K.N., Stacy, A.K., Bressler, D.A., Hayashi, L.S., Hengen, K.B., & Van Hooser, S.D. (2021). Construction and implementation of carbon fiber microelectrode arrays for chronic and acute in vivo recordings. Journal of Visual Experiments, 05 Aug 2021 (174). https://doi.org/10.3791/62760
23. Samejima, S., Caskey, C. D., Inanici, F., Shrivastav, S. R., Brighton, L. N., Pradarelli, J., Martinez, V., Steele, K. M., Saigal, R., & Moritz, C. T. (2022). Multisite Transcutaneous Spinal Stimulation for Walking and Autonomic Recovery in Motor-Incomplete Tetraplegia: A Single-Subject Design. Physical Therapy, 102(1), pzab228. https://doi.org/10.1093/ptj/pzab228
24. Shinozaki, M., Nagoshi, N., Nakamura, M., & Okano, H. (2021). Mechanisms of Stem Cell Therapy in Spinal Cord Injuries. Cells, 10(10), 2676. https://doi.org/10.3390/cells10102676
25. Steeves, J. D., Kramer, J. K., Fawcett, J. W., Cragg, J., Lammertse, D. P., Blight, A. R., Marino, R. J., Ditunno, J. F., Coleman, W. P., Geisler, F. H., Guest, J., Jones, L., Burns, S., Schubert, M., Van Hedel, H. J. A., & Curt, A. (2011). Extent of spontaneous motor

recovery after traumatic cervical sensorimotor complete spinal cord injury. Spinal Cord, 49(2), 257–265. https://doi.org/10.1038/sc.2010.99
26. Takeoka, A., & Arber, S. (2019). Functional Local Proprioceptive Feedback Circuits Initiate and Maintain Locomotor Recovery after Spinal Cord Injury. *Cell Reports*, *27*(1), 71-85.e3. https://doi.org/10.1016/j.celrep.2019.03.010
27. Venkatesh, I., Mehra, V., Wang, Z., Simpson, M. T., Eastwood, E., Chakraborty, A., Beine, Z., Gross, D., Cabahug, M., Olson, G., & Blackmore, M. G. (2020). Co-occupancy analysis reveals novel transcriptional synergies for axon growth [Preprint]. Neuroscience. https://doi.org/10.1101/2020.06.12.146159
28. Vipin, A., Thow, X. Y., Mir, H., Kortelainen, J., Manivannan, J., Al-Nashash, H., & All, A. H. (2016). Natural Progression of Spinal Cord Transection Injury and Reorganization of Neural Pathways. Journal of Neurotrauma, 33(24), 2191–2201. https://doi.org/10.1089/neu.2015.4383
29. Yang, F.-A., Chen, S.-C., Chiu, J.-F., Shih, Y.-C., Liou, T.-H., Escorpizo, R., & Chen, H.-C. (2022). Body weight-supported gait training for patients with spinal cord injury: A network meta-analysis of randomised controlled trials. Scientific Reports, 12(1), 19262. https://doi.org/10.1038/s41598-022-23873-8